arXiv:physics/0001065v1 [physics.acc-ph] 27 Jan 2000

Beam Coupling Impedances of Small Discontinuities*

Sergey S. Kurennoy
SNS Division, Los Alamos National Laboratory,
Los Alamos, NM 87545, USA

Abstract

A general derivation of the beam coupling impedances produced by small discontinuities on the wall of the vacuum chamber of an accelerator is reviewed. A collection of analytical formulas for the impedances of small obstacles is presented.

1 Introduction

A common tendency in design of modern accelerators is to minimize beam-chamber coupling impedances to avoid beam instabilities and reduce heating. Even contributions from tiny discontinuities like pumping holes have to be accounted for because of their large number. Numerical time-domain methods are rather involved and time-consuming for small obstacles, especially for those protruding inside the beam pipe. This makes analytical methods for calculating the impedances of small discontinuities very important.

A discontinuity on the wall of a beam pipe — a hole, cavity, post, mask, etc. — is considered to be small when its typical size is small compared to the size of the chamber cross section and the wavelength. Analytical calculations of the coupling impedances of small obstacles are based on the Bethe theory of diffraction of electromagnetic waves by a small hole in a metal plane [1]. The method's basic idea is that the hole in the frequency range where the wavelength is large compared to the typical hole size, can be replaced by two induced dipoles, an electric and a magnetic one. The dipole magnitudes are proportional to the beam fields at the hole location, with the coefficients called polarizabilities [2]. The fields diffracted by a hole into the vacuum chamber can be found as those radiated by these effective electric and magnetic dipoles, and integrating the fields gives us the coupling impedances. Following this path, the impedances produced by a small hole on the round pipe were calculated first in [3].

Since essentially the same idea works for any small obstacle, the method can be extended for arbitrary small discontinuities on the pipe with an arbitrary-shaped cross section. Analytical expressions for the coupling impedances of various small discontinuities on the wall of a cylindrical beam pipe with an arbitrary single-connected cross section have been obtained in Refs. [3]-[9].

All the dependence on the discontinuity shape enters only through its polarizabilities. Therefore, the problem of calculating the impedance contribution from a given small discontinuity was reduced to finding its electric and magnetic polarizabilities, which can be done by solving proper electro- or magnetostatic problem. Useful analytical results have been obtained for various axisymmetric obstacles (cavities and irises) [10], as well as for holes and slots: circular [1] and elliptic [2] hole in a zero-thickness wall, circular [11] and elliptic [12] hole in a thick wall, various slots (some results are compiled in [13]), and for a ring-shaped cut [14]. The impedances of various protrusions (post, mask, etc) have been calculated in [15].

This text is organized as follows. In Sections 2 and 3 a general derivation of the coupling impedances for a small discontinuity is given, and then in Sect. 4 the trapped modes are discussed. This part mostly follows Ref. [9]. In Sect. 5 we collected for the reader convenience some practical formulas for the coupling

*Lectures presented at the US Particle Accelerator School in Tucson, AZ on January 17-21, 2000, as a part of R.L. Gluckstern's course "Analytic Methods for Calculating Coupling Impedances"

impedances of various small discontinuities. In a compact form, many of these formulas are included in the handbook [16].

2 Fields

2.1 Beam Fields

Let us consider an infinite cylindrical pipe with an arbitrary cross section S and perfectly conducting walls. The z axis is directed along the pipe axis, a hole (or another small discontinuity like a post, cavity or mask) is located at the point $(\vec{b}, z = 0)$, and its typical size h satisfies $h \ll b$. To evaluate the coupling impedance one has to calculate the fields induced in the chamber by a given current. If an ultrarelativistic point charge q moves parallel to the chamber axis with the transverse offset $\vec{s}$ from the axis, the fields harmonics $\vec{E}^b, \vec{H}^b$ produced by this charge on the chamber wall without discontinuity would be

$$\begin{aligned} E^b_\nu(\vec{s}, z; \omega) &= Z_0 H^b_\tau(\vec{s}, z; \omega) \\ &= -Z_0 q e^{ikz} \sum_{n,m} k_{nm}^{-2} e_{nm}(\vec{s}) \nabla_\nu e_{nm}(\vec{b}) \ , \end{aligned} \tag{1}$$

where $Z_0 = 120\pi$ Ohms is the impedance of free space, and k^2_{nm}, $e_{nm}(\vec{r})$ are eigenvalues and orthonormalized eigenfunctions (EFs) of the 2D boundary problem in S:

$$\left(\nabla^2 + k^2_{nm}\right) e_{nm} = 0 \ ; \qquad e_{nm}\big|_{\partial S} = 0 \ . \tag{2}$$

Here $\vec{\nabla}$ is the 2D gradient in plane S; $k = \omega/c$; $\hat{\nu}$ means an outward normal unit vector, $\hat{\tau}$ is a unit vector tangent to the boundary ∂S of the chamber cross section S, and $\{\hat{\nu}, \hat{\tau}, \hat{z}\}$ form a right-handed basis. The differential operator ∇_ν is the scalar product $\nabla_\nu = \hat{\nu} \cdot \vec{\nabla}$. The eigenvalues and EFs for circular and rectangular cross sections are given in the Appendix.

Let us introduce the following notation for the sum in Eq. (1)

$$e_\nu(\vec{s}) = -\sum_g k_g^{-2} e_g(\vec{s}) \nabla_\nu e_g(\vec{b}) \tag{3}$$

where $g = \{n, m\}$ is a generalized index. From a physical viewpoint, this is just a normalized electrostatic field produced at the hole location by a filament charge displaced from the chamber axis by distance $\vec{s}$. It satisfies the normalization condition

$$\oint_{\partial S} dl \ e_\nu(\vec{s}) = 1 \ , \tag{4}$$

where integration goes along the boundary ∂S, which is a consequence of the Gauss law. It follows from the fact that Eq. (3) gives the boundary value of $\vec{e}_\nu(\vec{s}) \equiv -\vec{\nabla}\Phi(\vec{r} - \vec{s})$, where $\Phi(\vec{r} - \vec{s})$ is the Green function of boundary problem (2): $\nabla^2 \Phi(\vec{r} - \vec{s}) = -\delta(\vec{r} - \vec{s})$. For the symmetric case of an on-axis beam in a circular pipe of radius b from Eq. (4) immediately follows $e_\nu(0) = 1/(2\pi b)$. It can also be derived by directly summing up the series in Eq. (3) for this particular case.

2.2 Effective Dipoles and Polarizabilities

At distances l such that $h \ll l \ll b$, the fields radiated by the hole into the pipe are equal to those produced by effective dipoles [1, 2]

$$\begin{aligned} P_\nu &= -\chi \varepsilon_0 E^h_\nu / 2; \quad M_\tau = (\psi_{\tau\tau} H^h_\tau + \psi_{\tau z} H^h_z)/2; \\ M_z &= (\psi_{z\tau} H^h_\tau + \psi_{zz} H^h_z)/2 \ , \end{aligned} \tag{5}$$

where superscript 'h' means that the fields are taken at the hole. Polarizabilities ψ, χ are related to the effective ones α_e, α_m used in [2, 3] as $\alpha_e = -\chi/2$ and $\alpha_m = \psi/2$, so that for a circular hole of radius a in a thin wall $\psi = 8a^3/3$ and $\chi = 4a^3/3$ [1]. In general, ψ is a symmetric 2D-tensor, which can be diagonalized. If the hole is symmetric, and its symmetry axis is parallel to $\hat{z}$, the skew terms vanish, i.e. $\psi_{\tau z} = \psi_{z\tau} = 0$. In a more general case of a non-zero tilt angle α between the major symmetry axis and $\hat{z}$,

$$\begin{aligned} \psi_{\tau\tau} &= \psi_\perp \cos^2\alpha + \psi_\parallel \sin^2\alpha \ , \\ \psi_{\tau z} &= \psi_{z\tau} = (\psi_\parallel - \psi_\perp)\sin\alpha\cos\alpha \ , \\ \psi_{zz} &= \psi_\perp \sin^2\alpha + \psi_\parallel \cos^2\alpha \ , \end{aligned} \tag{6}$$

where $\psi_\parallel$ is the longitudinal magnetic susceptibility (for the external magnetic field along the major axis), and $\psi_\perp$ is the transverse one (the field is transverse to the major axis of the hole). When the effective dipoles are obtained, e.g., by substituting beam fields (1) into Eqs. (5), one can calculate the fields in the chamber as a sum of waveguide eigenmodes excited in the chamber by the dipoles, and find the impedance. This approach has been carried out for a circular pipe in [3], and for an arbitrary chamber in [5]. The polarizabilities for various types of small discontinuities are discussed in detail in Section 5.

2.3 Radiated Fields

The radiated fields in the chamber can be expanded in a series in TM- and TE-eigenmodes [2] as

$$\begin{aligned} \vec{F} = \sum_{nm} \Big[A^+_{nm} \vec{F}^{(E)+}_{nm} \theta(z) + A^-_{nm} \vec{F}^{(E)-}_{nm} \theta(-z) \Big] + \\ \sum_{nm} \Big[B^+_{nm} \vec{F}^{(H)+}_{nm} \theta(z) + B^-_{nm} \vec{F}^{(H)-}_{nm} \theta(-z) \Big] \ , \end{aligned} \tag{7}$$

where $\vec{F}$ means either $\vec{E}$ or $\vec{H}$, superscripts '$\pm$' denote waves radiated respectively in the positive ($+$, $z > 0$) or negative ($-$, $z < 0$) direction, and $\theta(z)$ is the Heaviside step function. The fields $F^{(E)}_{nm}$ of $\{n, m\}$th TM-eigenmode in Eq. (7) are expressed [2] in terms of EFs (2)

$$\begin{aligned} E^\mp_z &= k^2_{nm} e_{nm} \exp(\pm\Gamma_{nm} z) \ ; \qquad H^\mp_z = 0 \ ; \\ \vec{E}^\mp_t &= \pm\Gamma_{nm} \vec{\nabla} e_{nm} \exp(\pm\Gamma_{nm} z) \ ; \\ \vec{H}^\mp_t &= \frac{ik}{Z_0} \hat{z} \times \vec{\nabla} e_{nm} \exp(\pm\Gamma_{nm} z) \ , \end{aligned} \tag{8}$$

where propagation factors $\Gamma_{nm} = (k^2_{nm} - k^2)^{1/2}$ should be replaced by $-i\beta_{nm}$ with $\beta_{nm} = (k^2 - k^2_{nm})^{1/2}$ for $k > k_{nm}$. For given values of dipoles (5) the unknown coefficients $A^\pm_{nm}$ can be found [3, 5] using the Lorentz reciprocity theorem

$$A^\pm_{nm} = a_{nm} M_\tau \pm b_{nm} P_\nu \ , \tag{9}$$

with

$$a_{nm} = -\frac{ikZ_0}{2\Gamma_{nm} k^2_{nm}} \nabla_\nu e^h_{nm} \ ; \quad b_{nm} = \frac{1}{2\varepsilon_0 k^2_{nm}} \nabla_\nu e^h_{nm} \ . \tag{10}$$

The fields $F^{(H)}_{nm}$ of the TE$_{nm}$-eigenmode in Eq. (7) are

$$\begin{aligned} H^\mp_z &= k'^2_{nm} h_{nm} \exp(\pm\Gamma'_{nm} z) \ ; \qquad E^\mp_z = 0 \ ; \\ \vec{H}^\mp_t &= \pm\Gamma'_{nm} \vec{\nabla} h_{nm} \exp(\pm\Gamma'_{nm} z) \ ; \\ \vec{E}^\mp_t &= -ikZ_0 \hat{z} \times \vec{\nabla} h_{nm} \exp(\pm\Gamma'_{nm} z) \ , \end{aligned} \tag{11}$$

with propagation factors $\Gamma'_{nm} = (k'^2_{nm} - k^2)^{1/2}$ replaced by $-i\beta'_{nm} = -i(k^2 - k'^2_{nm})^{1/2}$ when $k > k'_{nm}$. Here EFs h_{nm} satisfy the boundary problem (2) with the Neumann boundary condition $\nabla_\nu h_{nm}|_{\partial S} = 0$, and k'^2_{nm}

are corresponding eigenvalues, see in Appendix. The TE-mode excitation coefficients in the expansion (7) for the radiated fields are

$$B^{\pm}_{nm} = \pm c_{nm} M_\tau + d_{nm} P_\nu + q_{nm} M_z \ , \tag{12}$$

where

$$\begin{aligned} c_{nm} &= \frac{1}{2k'^2_{nm}} \nabla_\tau h^h_{nm} \ ; \quad q_{nm} = \frac{1}{2\Gamma'_{nm}} h^h_{nm} \ ; \\ d_{nm} &= -\frac{ik}{2Z_0 \varepsilon_0 \Gamma'_{nm} k'^2_{nm}} \nabla_\tau h^h_{nm} \ . \end{aligned} \tag{13}$$

2.4 Fields near Hole with Radiation Corrections

A more refined theory should take into account the reaction of radiated waves back on the hole. Adding corrections to the beam fields (1) due to the radiated waves in the vicinity of the hole gives

$$E_\nu = \frac{E^b_\nu + \psi_{z\tau} \Sigma'_x Z_0 H_\tau + \psi_{zz} \Sigma'_x Z_0 H_z}{1 - \chi(\Sigma_1 - \Sigma'_1)}, \tag{14}$$

$$H_\tau = \frac{H^b_\tau + \psi_{\tau z}(\Sigma_2 - \Sigma'_2) H_z}{1 - \psi_{\tau\tau}(\Sigma_2 - \Sigma'_2)}, \tag{15}$$

$$H_z = \frac{\chi \Sigma'_x E_\nu / Z_0 + \psi_{z\tau} \Sigma'_3 H_\tau}{1 - \psi_{zz} \Sigma'_3}, \tag{16}$$

where ($s = \{n, m\}$ is a generalized index)

$$\begin{aligned} \Sigma_1 &= \frac{1}{4} \sum_s \frac{\Gamma_s \left(\nabla_\nu e^h_s\right)^2}{k^2_s} \ ; \ \Sigma_2 = \frac{k^2}{4} \sum_s \frac{\left(\nabla_\nu e^h_s\right)^2}{\Gamma_s k^2_s} \ ; \\ \Sigma'_1 &= \frac{k^2}{4} \sum_s \frac{\left(\nabla_\tau h^h_s\right)^2}{\Gamma'_s k'^2_s} \ ; \ \Sigma'_2 = \frac{1}{4} \sum_s \frac{\Gamma'_s \left(\nabla_\tau h^h_s\right)^2}{k'^2_s} \ ; \\ \Sigma'_x &= i \frac{k}{4} \sum_s \frac{h^h_s \nabla_\tau h^h_s}{\Gamma'_s} \ ; \ \Sigma'_3 = \frac{1}{4} \sum_s \frac{k'^2_s \left(h^h_s\right)^2}{\Gamma'_s} \ . \end{aligned} \tag{17}$$

Since this consideration works at distances larger than h, one should restrict the summation in Eq. (17) to the values of $s = \{n, m\}$ such that $k_s h \leq 1$ and $k'_s h \leq 1$.

3 Impedance

3.1 Longitudinal Impedance

The generalized longitudinal impedance of the hole depends on the transverse offsets from the chamber axis $\vec{s}$ of the leading particle and $\vec{t}$ of the test particle, and is defined [6] as

$$Z(k; \vec{s}, \vec{t}\,) = -\frac{1}{q} \int_{-\infty}^{\infty} dz e^{-ikz} E_z(\vec{t}, z; \omega) \ , \tag{18}$$

where the longitudinal field $E_z(\vec{t}, z; \omega)$ is taken along the test particle path. The displacements from the axis are assumed to be small, $s \ll b$ and $t \ll b$. The impedance $Z(k; \vec{s}, \vec{t}\,)$ includes higher multipole longitudinal impedances, and in the limit $s, t \to 0$ gives the usual monopole one $Z(k) = Z(k; 0, 0)$. To calculate $E_z(\vec{t}, z; \omega)$,

we use Eq. (7) with coefficients (9) and (12) in which the corrected near-hole fields (14)-(16) are substituted [a dependence on $\vec{s}$ enters via beam fields (1)]. It yields

$$Z(k;\vec{s},\vec{t}\,) = -\frac{ikZ_0 e_\nu(\vec{s}\,)e_\nu(\vec{t}\,)}{2} \times \qquad (19)$$
$$\times \left[\frac{\psi_{\tau\tau}}{1-\psi_{\tau\tau}(\Sigma_2-\Sigma_2')} + \psi_{\tau z}^2\Sigma_3' - \frac{\chi}{1-\chi(\Sigma_1-\Sigma_1')} \right] ,$$

where $e_\nu(\vec{r}\,)$ is defined above by Eq. (3). In practice, we are usually interested only in the monopole term $Z(k) = Z(k;0,0)$, and will mostly use Eq. (19) with replacement $e_\nu(\vec{s}\,)e_\nu(\vec{t}\,) \to \tilde{e}_\nu^2$, where $\tilde{e}_\nu \equiv e_\nu(0)$. In deriving Eq. (19) we have neglected the coupling terms between E_ν, H_τ and H_z, cf. Eqs. (14)-(16), which contribute to the third order of an expansion discussed below, and also have taken into account that $\psi_{\tau z} = \psi_{z\tau}$.

For a small discontinuity, polarizabilities $\psi, \chi = O(h^3)$, and they are small compared to b^3. If we expand the impedance (19) in a perturbation series in polarizabilities, the first order gives

$$Z_1(k) = -\frac{ikZ_0\tilde{e}_\nu^2}{2}\left(\psi_{\tau\tau} - \chi\right) , \qquad (20)$$

that is exactly the inductive impedance obtained in [5] for an arbitrary cross section of the chamber. For a particular case of a circular pipe, from either direct summation in (1) or applying the Gauss law, one gets $\tilde{e}_\nu = 1/(2\pi b)$. Substituting that into Eq. (20) leads to a well-known result [3, 4]:

$$Z(k) = -ikZ_0\frac{\psi_{\tau\tau}-\chi}{8\pi^2 b^2} = -ikZ_0\frac{\alpha_e+\alpha_m}{4\pi^2 b^2} , \qquad (21)$$

where we recall that two definitions of the polarizabilities are related as $\alpha_e = -\chi/2$ and $\alpha_m = \psi_{\tau\tau}/2$.

From a physical point of view, keeping only the first order term (20) corresponds to dropping out all radiation corrections in Eqs. (14)-(16). These corrections first reveal themselves in the second order term

$$Z_2(k) = -\frac{ikZ_0\tilde{e}_\nu^2}{2}\left[\psi_{\tau\tau}^2(\Sigma_2-\Sigma_2') + \psi_{\tau z}^2\Sigma_3' + \chi^2(\Sigma_1'-\Sigma_1)\right] , \qquad (22)$$

which at frequencies above the chamber cutoff has both a real and imaginary part. The real part of the impedance is

$$\begin{aligned} ReZ_2(k) &= \frac{k^3 Z_0\tilde{e}_\nu^2}{8}\left\{\psi_{\tau z}^2\sum_s^{<}\frac{k_s'^2\left(h_s^h\right)^2}{k^2\beta_s'}\right. \qquad (23)\\ &+ \psi_{\tau\tau}^2\left[\sum_s^{<}\frac{\left(\nabla_\nu e_s^h\right)^2}{\beta_s k_s^2} + \sum_s^{<}\frac{\beta_s'\left(\nabla_\tau h_s^h\right)^2}{k^2 k_s'^2}\right]\\ &+ \left.\chi^2\left[\sum_s^{<}\frac{\beta_s\left(\nabla_\nu e_s^h\right)^2}{k^2 k_s^2} + \sum_s^{<}\frac{\left(\nabla_\tau h_s^h\right)^2}{\beta_s' k_s'^2}\right]\right\} , \end{aligned}$$

where the sums include only a finite number of the eigenmodes propagating in the chamber at a given frequency, i.e. those with $k_s < k$ or $k_s' < k$.

The dependence of $Re\,Z$ on frequency is rather complicated; it has sharp peaks near the cutoffs of all propagating eigenmodes of the chamber, and increases in average with the frequency increase. Well above the chamber cutoff, i.e. when $kb \gg 1$ (but still $kh \ll 1$ to justify the Bethe approach), this dependence can be derived as follows. If the waveguide cross section S is a simply connected region, the average number $n(k)$ of the eigenvalues k_s (or k_s') which are less than k, for $kb \gg 1$, is proportional to k^2 [17]:

$$n(k) \simeq \frac{S}{4\pi}k^2 + O(k) ,$$

where S is the area of the cross section. Using this property, and taking into account that $\nabla_\nu e_s^h \propto k_s e_s^h$, and $\nabla_\tau h_s^h \propto k_s' h_s^h$, we replace sums in the RHS of Eq. (23) by integrals as $\sum_s^< \to \int^k dk \frac{d}{dk} n(k)$. It turns out that all sums in Eq. (23) have the same asymptotic behavior, being linear in k, and as a result, $Re\, Z \propto k^4$. Obtaining the exact coefficient in this dependence seems rather involved for a general S, but it can be easily done for a rectangular chamber, see in Appendix B. The result is

$$Re\, Z = \frac{Z_0 k^4 \tilde{e}_\nu^2}{12\pi} (\psi_{\tau\tau}^2 + \psi_{\tau z}^2 + \chi^2) \ . \tag{24}$$

Remarkably, the same answer (for $\psi_{\tau z} = 0$) has been obtained in Ref. [3] simply by calculating the energy radiated by the dipoles into a half-space. The physical reason for this coincidence is clear: at frequencies well above the cutoff the effective dipoles radiate into the waveguide the same energy as into an open half-space.

Strictly speaking, the real part of impedance is non-zero even below the chamber cutoff, due to radiation outside. In the case of a thin wall, $Re\, Z$ below the cutoff can be estimated by Eq. (24), and twice that for high frequencies, $kb \gg 1$. For a thick wall, the contribution of the radiation outside to $Re\, Z$ is still given by Eq. (24), but with the outside polarizabilities substituted, and it decreases exponentially with the thickness increase [4].

The real part of the impedance is related to the power P scattered by the hole into the beam pipe as $Re\, Z = 2P/q^2$. These energy considerations can be used as an alternative way for the impedance calculation. The radiated power is

$$P = \sum_s \left[A_s^2 P_s^{(E)} + B_s^2 P_s^{(H)} \right] \ ,$$

where we sum over all propagating modes in both directions, and P_s means the time-averaged power radiated in sth eigenmode:

$$P_s^{(E)} = k\beta_s k_s^2/(2Z_0) \quad \text{and} \quad P_s^{(H)} = Z_0 k \beta_s' k_s'^2/2 \ .$$

Substituting beam fields (1) into Eqs. (9)-(13) for the coefficients A_s and B_s and performing calculations gives us exactly the result (23). Such an alternative derivation of the real part has been carried out in Ref. [8] for a circular pipe with a symmetric untilted hole ($\psi_{\tau z} = 0$). Our result (23) coincides, in this particular case, with that of Reference [8]. It is appropriate to mention also that in this case at high frequencies the series has been summed approximately [8] using asymptotic expressions for roots of the Bessel functions, and the result, of course, agrees with Eq. (24).

One should note that the additional $\psi_{\tau z}^2$-term in Eq. (23) is important in some particular cases. For example, this skew term gives a leading contribution to $Re\, Z$ for a long and slightly tilted slot, because $\psi_{\tau z}$ can be much larger than $\psi_{\tau\tau}$ in this case, since $\psi_\parallel \gg \psi_\perp$, cf. Eqs. (6).

3.2 Transverse Impedance

We will make use of the expression for the generalized longitudinal impedance $Z(k; \vec{s}, \vec{t})$, Eq. (19). According to the Panofsky-Wenzel theorem, the transverse impedance can be derived as $\vec{Z}_\perp(k; \vec{s}, \vec{t}) = \vec{\nabla} Z(k; \vec{s}, \vec{t})/(ks)$, see, e.g., [6] for details. This way leads to the expression

$$\vec{Z}_\perp(k; \vec{s}, \vec{t}) = -\frac{iZ_0 e_\nu^{dip}(\vec{s}) \vec{\nabla} e_\nu(\vec{t})}{2s} \times \tag{25}$$
$$\times \left[\frac{\psi_{\tau\tau}}{1 - \psi_{\tau\tau}(\Sigma_2 - \Sigma_2')} + \psi_{\tau z}^2 \Sigma_3' - \frac{\chi}{1 - \chi(\Sigma_1 - \Sigma_1')} \right] \ ,$$

where $e_\nu^{dip}(\vec{s}) = \vec{s} \cdot \vec{\nabla} e_\nu(\vec{s})$.

Going to the limit $s \to t \to 0$, we get the usual dipole transverse impedance

$$\vec{Z}_\perp(k) = -iZ_0 \frac{1}{2} (d_x^2 + d_y^2)\ \vec{a}_d \cos(\varphi_b - \varphi_d) \times \tag{26}$$
$$\times \left[\frac{\psi_{\tau\tau}}{1 - \psi_{\tau\tau}(\Sigma_2 - \Sigma_2')} + \psi_{\tau z}^2 \Sigma_3' - \frac{\chi}{1 - \chi(\Sigma_1 - \Sigma_1')} \right] \ .$$

Here x, y are the horizontal and vertical coordinates in the chamber cross section; $d_x \equiv \partial_x e_\nu(0)$, $d_y \equiv \partial_y e_\nu(0)$; $\varphi_b = \varphi_s = \varphi_t$ is the azimuthal angle of the beam position in the cross-section plane; $\vec{a}_d = \vec{a}_x \cos\varphi_d + \vec{a}_y \sin\varphi_d$ is a unit vector in this plane in direction φ_d, which is defined by conditions $\cos\varphi_d = d_x/\sqrt{d_x^2 + d_y^2}$, $\sin\varphi_d = d_y/\sqrt{d_x^2 + d_y^2}$. It is seen from Eq. (26) that the angle φ_d shows the direction of the transverse-impedance vector $\vec{Z}_\perp$ and, therefore, of the beam-deflecting force. Moreover, the value of $Z_\perp$ is maximal when the beam is deflected along this direction and vanishes when the beam offset is perpendicular to it.

The equation (26) includes the corrections due to waves radiated by the hole into the chamber in exactly the same way as Eq. (19) for the longitudinal impedance. If we expand it in a series in the polarizabilities, the first order of the square brackets in (26) gives $(\psi_{\tau\tau} - \chi)$, and the resulting inductive impedance is [5]:

$$\vec{Z}_\perp(k) = -iZ_0 \frac{1}{2}(d_x^2 + d_y^2)\ \vec{a}_d \cos(\varphi_b - \varphi_d)\,(\psi_{\tau\tau} - \chi)\ . \tag{27}$$

For a circular pipe, $d_x = \cos\varphi_h/(\pi b^2)$ and $d_y = \sin\varphi_h/(\pi b^2)$, where φ_h is the azimuthal position of the discontinuity (hole). As a result, $\varphi_d = \varphi_h$, and the deflecting force is directed toward (or opposite to) the hole. Note that in axisymmetric structures the beam-deflecting force is directed along the beam offset; the presence of an obstacle obviously breaks this symmetry. For a general cross section, the direction of the deflecting force depends on the hole position in a complicated way, see [5] for rectangular and elliptic chambers.

The transverse impedance of a discontinuity on the wall of a circular pipe has a simple form [3]:

$$\vec{Z}_{\perp\, circ}(k) = -iZ_0 \frac{\psi_{\tau\tau} - \chi}{2\pi^2 b^4}\ \vec{a}_h \cos(\varphi_b - \varphi_d) = -iZ_0 \frac{\alpha_m + \alpha_e}{\pi^2 b^4}\ \vec{a}_h \cos(\varphi_b - \varphi_d)\ , \tag{28}$$

where $\vec{a}_h$ is a unit vector in the direction from the chamber axis to the discontinuity, orthogonal to $\hat{z}$.

For M ($M \geq 3$) holes uniformly spaced in one cross section of a circular beam pipe, a vector sum of M expressions (28) gives the transverse impedance as

$$\vec{Z}_{\perp\, circ\ M}(k) = -iZ_0 \frac{\alpha_m + \alpha_e}{\pi^2 b^4} \frac{M}{2} \vec{a}_b\ , \tag{29}$$

where $\vec{a}_b = \vec{s}/|\vec{s}|$ is a unit vector in the direction of the beam transverse offset. One can see that the deflecting force is now directed along the beam offset, i.e. some kind of the axial symmetry restoration occurs. The maximal value of $Z_\perp$ for M holes which are uniformly spaced in one cross-section is only $M/2$ times larger than that for $M = 1$. Moreover, the well-known empirical relation $Z_\perp = (2/b^2 k)Z$, which is justified only for axisymmetric structures, holds in this case also.

The second order term in Eq. (26) includes $Re\, Z_\perp$, cf. Sect. 3.1 for the longitudinal impedance.

4 Trapped Modes

So far we considered the perturbation expansion of Eq. (19) implicitly assuming that correction terms $O(\psi)$ and $O(\chi)$ in the denominators of its right-hand side (RHS) are small compared to 1. Under certain conditions this assumption is incorrect, and it leads to some non-perturbative results. Indeed, at frequencies slightly below the chamber cut-offs, $0 < k_s - k \ll k_s$ (or the same with replacement $k_s \to k'_s$), a single term in sums Σ'_1, Σ_2, or Σ'_3 becomes very large, due to very small $\Gamma_s = (k_s^2 - k^2)^{1/2}$ (or Γ'_s) in its denominator, and then the "corrections" $\psi\Sigma$ or $\chi\Sigma$ can be of the order of 1. As a result, one of the denominators of the RHS of Eqs. (19) can vanish, which corresponds to a resonance of the coupling impedance. On the other hand, vanishing denominators in Eqs. (14)-(16) mean the existence of non-perturbative eigenmodes of the chamber with a hole, since non-trivial solutions $E, H \neq 0$ exist even for vanishing external (beam) fields $E^b, H^b = 0$. These eigenmodes are nothing but the trapped modes studied in [18] for a circular waveguide with a small discontinuity. In our approach, one can easily derive parameters of trapped modes for waveguides with an arbitrary cross section.

4.1 Frequency Shifts

Let us for brevity restrict ourselves to the case $\psi_{\tau z} = 0$ and consider Eq. (15) in more detail. For $H^b = 0$ we have

$$H_\tau \left[1 - \psi_{\tau\tau} \frac{k^2 \left(\nabla_\nu e_s^h \right)^2}{4\Gamma_s k_s^2} + \dots \right] = 0 \ , \tag{30}$$

where $s \equiv \{nm\}$ is the generalized index, and $\dots$ mean all other terms of the series Σ_2, Σ_2'. At frequency Ω_s slightly below the cutoff frequency $\omega_s = k_s c$ of the TM_s-mode, the fraction in Eq. (30) is large due to small Γ_s in its denominator, and one can neglect the other terms. Then the condition for a non-trivial solution $H_\tau \neq 0$ to exist is

$$\Gamma_s \simeq \frac{1}{4} \psi_{\tau\tau} \left(\nabla_\nu e_s^h \right)^2 \ . \tag{31}$$

In other words, there is a solution of the homogeneous, i.e., without external currents, Maxwell equations for the chamber with the hole, having the frequency $\Omega_s < \omega_s$ — the sth trapped TM-mode. When Eq. (31) is satisfied, the series (7) is obviously dominated by the single term $A_s F_s^E$; hence, the fields of the trapped mode have the form [cf. Eq. (8)]

$$\begin{aligned} \mathcal{E}_z &= k_s^2 e_s \exp(-\Gamma_s |z|) \ ; \qquad \mathcal{H}_z = 0 \ ; \\ \vec{\mathcal{E}}_t &= \mathrm{sgn}(z) \Gamma_s \vec{\nabla} e_s \exp(-\Gamma_s |z|) \ ; \\ Z_0 \vec{\mathcal{H}}_t &= ik\hat{z} \times \vec{\nabla} e_s \exp(-\Gamma_s |z|) \ , \end{aligned} \tag{32}$$

up to some arbitrary amplitude. Strictly speaking, these expressions are valid at distances $|z| > b$ from the discontinuity. Typically, $\psi_{\tau\tau} = O(h^3)$ and $\nabla_\nu e_s^h = O(1/b)$, and, as a result, $\Gamma_s b \ll 1$. It follows that the field of the trapped mode extends along the vacuum chamber over the distance $1/\Gamma_s$, large compared to the chamber transverse dimension b.

The existence of the trapped modes in a circular waveguide with a small hole was first proved in [18], and conditions similar to Eq. (31) for this particular case were obtained in [18, 19], using the Lorentz reciprocity theorem. From the general approach presented here for the waveguide with an arbitrary cross section, their existence follows in a natural way. Moreover, in such a derivation, the physical mechanism of this phenomenon becomes quite clear: a tangential magnetic field induces a magnetic moment on the hole, and the induced magnetic moment supports this field if the resonance condition (31) is satisfied, so that the mode can exist even without an external source. One should also note that the induced electric moment P_ν is negligible for the trapped TM-mode, since $P_\nu = O(\Gamma_s b) M_\tau$, as follows from Eq. (32).

The equation (31) gives the frequency shift $\Delta\omega_s \equiv \omega_s - \Omega_s$ of the trapped sth TM-mode down from the cutoff ω_s

$$\frac{\Delta\omega_s}{\omega_s} \simeq \frac{1}{32 k_s^2} \psi_{\tau\tau}^2 \left(\nabla_\nu e_s^h \right)^4 \ . \tag{33}$$

In the case of a small hole this frequency shift is very small, and for the trapped mode (32) to exist, the width of the resonance should be smaller than $\Delta\omega_s$. Contributions to the resonance width come from energy dissipation in the waveguide wall due to its finite conductivity, and from energy radiation inside the waveguide and outside, through the hole. Radiation escaping through the hole is easy to estimate [18], and for a thick wall it is exponentially small, e.g., [4]. The damping rate due to a finite conductivity is $\gamma = P/(2W)$, where P is the time-averaged power dissipation and W is the total field energy in the trapped mode, which yields

$$\frac{\gamma_s}{\omega_s} = \frac{\delta}{4 k_s^2} \oint dl \left(\nabla_\nu e_s \right)^2 \ , \tag{34}$$

where δ is the skin-depth at frequency Ω_s, and the integration is along the boundary ∂S. The evaluation of the radiation into the lower waveguide modes propagating in the chamber at given frequency Ω_s is also straightforward [8], if one makes use of the coefficients of mode excitation by effective dipoles on the hole, Eqs. (9)-(13). The corresponding damping rate $\gamma_R = O(\psi^3)$ is small compared to $\Delta\omega_s$. For instance, if there

is only one TE_p-mode with the frequency below that for the lowest TM_s-mode, like in a circular waveguide (H_{11} has a lower cutoff than E_{01}),

$$\frac{\gamma_R}{\Delta\omega_s} = \frac{\psi_{\tau\tau}\beta'_p}{k'^2_p}\left(\nabla_\nu h^h_s\right)^2 \ , \tag{35}$$

where $\beta'_p \simeq (k_s^2 - k'^2_p)^{1/2}$ because $k \simeq k_s$.

One can easily see that denominator $[1-\chi(\Sigma_1-\Sigma'_1)]$ in Eq. (14) does not vanish because singular terms in Σ'_1 have a "wrong" sign. However, due to the coupling between E_ν and H_z, a non-trivial solution $E_\nu, H_z \neq 0$ of simultaneous equations (14) and (16) can exist, even when $E^b = 0$. The corresponding condition has the form

$$\Gamma'_{nm} \simeq \frac{1}{4}\left[\psi_{zz}k'^2_{nm}\left(h^h_{nm}\right)^2 - \chi\left(\nabla_\tau h^h_{nm}\right)^2\right] \ , \tag{36}$$

which gives the frequency of the trapped TE_{nm}-mode, provided the RHS of Eq. (36) is positive.

4.2 Impedance

The trapped mode (32) gives a resonance contribution to the longitudinal coupling impedance at $\omega \approx \Omega_s$

$$Z_s(\omega) = \frac{2i\Omega_s\gamma_s R_s}{\omega^2 - (\Omega_s - i\gamma_s)^2} \ , \tag{37}$$

where the shunt impedance R_s can be calculated as that for a cavity with given eigenmodes, e.g. [6],

$$R_s = \frac{\sigma\delta\left|\int dz \exp(-i\Omega_s z/c)\mathcal{E}_z(z)\right|^2}{\int_{S_w} ds|\mathcal{H}_\tau|^2} \ . \tag{38}$$

The integral in the denominator is taken over the inner wall surface, and we assume here that the power losses due to its finite conductivity dominate. Integrating in the numerator one should include all TM-modes generated by the effective magnetic moment on the hole using Eqs. (9)-(13), in spite of a large amplitude of only the trapped TM_s mode. While all other amplitudes are suppressed by factor $\Gamma_s b \ll 1$, their contributions are comparable to that from TM_s, because this integration produces the factor $\Gamma_q b$ for any TM_q mode. The integral in the denominator is obviously dominated by TM_s. Performing calculations yields

$$R_s = \frac{Z_0\tilde{e}^2_\nu\psi^3_{\tau\tau}k_s\left(\nabla_\nu e^h_s\right)^4}{8\delta\oint dl\left(\nabla_\nu e_s\right)^2} \ , \tag{39}$$

where $\tilde{e}_\nu = e_\nu(0)$ is defined by Eq. (3).

Results for a particular shape of the chamber cross section can be obtained from the equations above by substituting the corresponding eigenfunctions (see Appendix).

One should note that typically the peak value R_s of the impedance resonance due to one small hole is rather small except for the limit of a perfectly conducting wall, $\delta \to 0$ — indeed, $R_s \propto (h/b)^9 b/\delta$, and $h \ll b$. However, for many not-so-far separated holes, the resulting impedance can be much larger. The trapped modes for many discontinuities on a circular waveguide has been studied in Ref. [19], and the results can be readily transferred to the considered case of an arbitrary shape of the chamber cross section. In particular, it was demonstrated that the resonance impedance in the extreme case can be as large as N^3 times that for a single discontinuity, where N is the number of discontinuities. It strongly depends on the distribution of discontinuities, or on the distance between them if a regular array is considered.

After the trapped modes in beam pipes with small holes were predicted theoretically [18, 19], their existence was proved by experiments with perforated waveguides at CERN [20].

5 Analytical Formulae for Some Small Discontinuities

For reader convenience, in this section we collected analytical expressions for the coupling impedances of various small discontinuities. The expressions give the inductive part of the impedance and work well at frequencies below the chamber cutoff, and, in many cases, even at much higher frequencies. However, there can also exist resonances of the real part at frequencies near the cutoff for holes and cavities due to the trapped modes, as was shown in [18, 19], and the real part of the impedance due to the energy radiated into the beam pipe should be taken into account at frequencies above the cutoff, see [7, 9, 21].

It is worth noting that both the longitudinal and transverse impedance are proportional to the same combination of polarizabilities, $\alpha_e + \alpha_m$, for any cross section of the beam pipe. Here we use the effective polarizabilities α_e, α_m as defined in [2]; they are related to the magnetic susceptibility ψ and the electric polarizability χ of an obstacle as $\alpha_e = -\chi/2$ and $\alpha_m = \psi/2$. The real part of the impedance is proportional to $\alpha_e^2 + \alpha_m^2$, and is usually small compared to the reactance at frequencies below the chamber cutoff. While the impedances below are written for a round pipe, more results for the other chamber cross sections, the impedance dependence on the obstacle position on the wall and on the beam position can be found in [5, 7, 9, 21, 22].

The longitudinal impedance of a small obstacle on the wall of a cylindrical beam pipe with a circular transverse cross section of radius R is simply [3] (up to notations, it is the same Eq. (21) above)

$$Z(k) = -ikZ_0 \frac{\alpha_e + \alpha_m}{4\pi^2 R^2} \ , \tag{40}$$

where $Z_0 = 120\pi$ Ohms is the impedance of free space, $k = \omega/c$ is the wave number, and α_e, α_m are the electric and magnetic polarizabilities of the discontinuity. The polarizabilities depend on the obstacle shape and size.

The transverse dipole impedance of the discontinuity for this case is

$$\vec{Z}_\perp(\omega) = -iZ_0 \frac{\alpha_m + \alpha_e}{\pi^2 R^4} \vec{a}_h \cos(\varphi_h - \varphi_b) \ , \tag{41}$$

where $\vec{a}_h$ is the unit vector directed to the obstacle in the chamber transverse cross section containing it, φ_h and φ_b are azimuthal angles of the obstacle and beam in this cross section.

5.1 Holes and Slots

For a circular hole with radius a in a thin wall, when thickness $t \ll a$, the polarizabilities are $\alpha_m = 4a^3/3$, $\alpha_e = -2a^3/3$, so that the impedance Eq. (40) takes a simple form

$$Z(k) = -ikZ_0 \frac{a^3}{6\pi^2 R^2} \ , \tag{42}$$

and similarly for Eq. (41). For the hole in a thick wall, $t \geq a$, the sum $(\alpha_m + \alpha_e) = 2a^3/3$ should be multiplied by a factor 0.56, see [4, 11]. There are also analytical expressions for polarizabilities of elliptic holes in a thin wall [2], and paper [12] gives thickness corrections for this case. Surprisingly, the thickness factor for $(\alpha_m + \alpha_e)$ exhibits only a weak dependence on ellipse eccentricity ε, changing its limiting value for the thick wall from 0.56 for $\varepsilon = 0$ to 0.59 for $\varepsilon = 0.99$.

For a longitudinal slot of length l and width w, $w/l \leq 1$, in a thin wall, useful approximations have been obtained [13]: for a rectangular slot

$$\alpha_m + \alpha_e = w^3(0.1814 - 0.0344w/l) \ ;$$

and for a rounded end slot

$$\alpha_m + \alpha_e = w^3(0.1334 - 0.0500w/l) \ ;$$

substituting of which into Eqs. (40)-(41) gives the impedances of slots. Figure 1 compares impedances for different shapes of pumping holes.

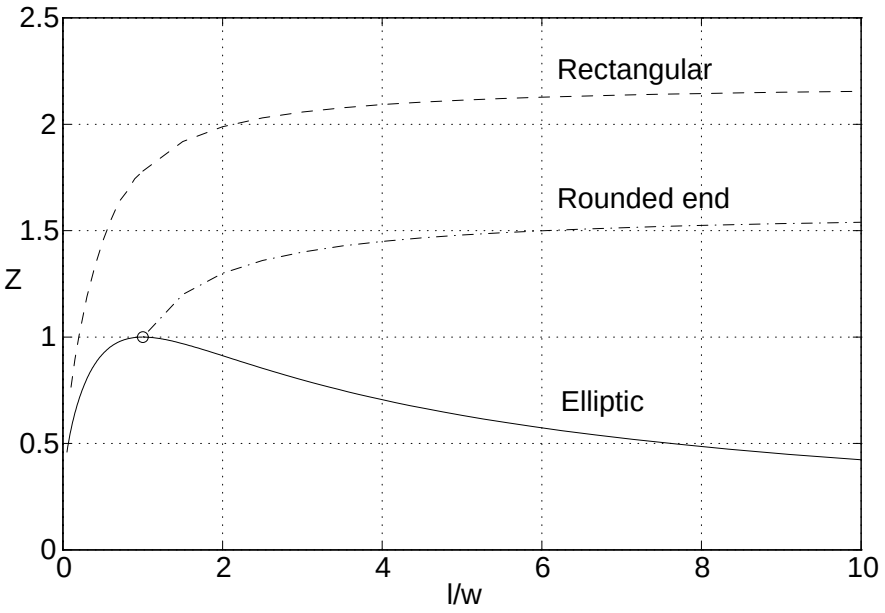

Figure 1: Slot impedance versus slot length l for fixed width w in units of the impedance of the circular hole with diameter w.

5.2 Annular Cut

The polarizabilities of a ring-shaped cut in the wall of an arbitrary thickness have been calculated in [14]. Such an aperture can serve as an approximation for a electrode of a button-type beam position monitor, for a thin wall, or a model of a coax attached to the vacuum chamber, when the wall thickness is large. If a and b denote the inner and outer radii of the annular cut, $a \leq b \ll R$, the magnetic susceptibility of a narrow ($w = b - a \ll b$) annular slot in a thin plate is

$$\psi \simeq \frac{\pi^2 b^2 a}{\ln(32b/w) - 2} \ . \tag{43}$$

For a narrow annular gap in the thick wall the asymptotic behavior is $\psi \simeq 2\pi b^2 w$. The approximation (43) works well for narrow gaps, $w/b \leq 0.15$, while the thick wall result is good only for $w/b \leq 0.05$.

Analytical results for the electric polarizability of a narrow annular cut are: for a thin wall

$$\chi \simeq \pi^2 w^2 (b + a)/8 \ , \tag{44}$$

and for a thick wall

$$\chi \simeq w^2 (b + a) \ . \tag{45}$$

These estimates work amazingly well even for very wide gaps, up to $w/b \geq 0.85$. The electric polarizability depends on the wall thickness rather weakly.

The difference $(\psi - \chi)/b^3 = 2(\alpha_m + \alpha_e)/b^3$ for an annular cut, calculated by variational methods in [14], is plotted in Fig. 2 for a few values of the wall thickness.

5.3 Protrusions

For a protrusion inside the beam pipe having the shape of a half ellipsoid with semiaxis a in the longitudinal direction (along the chamber axis), b in the radial direction, and c in the azimuthal one, with $a, b, c \ll R$,

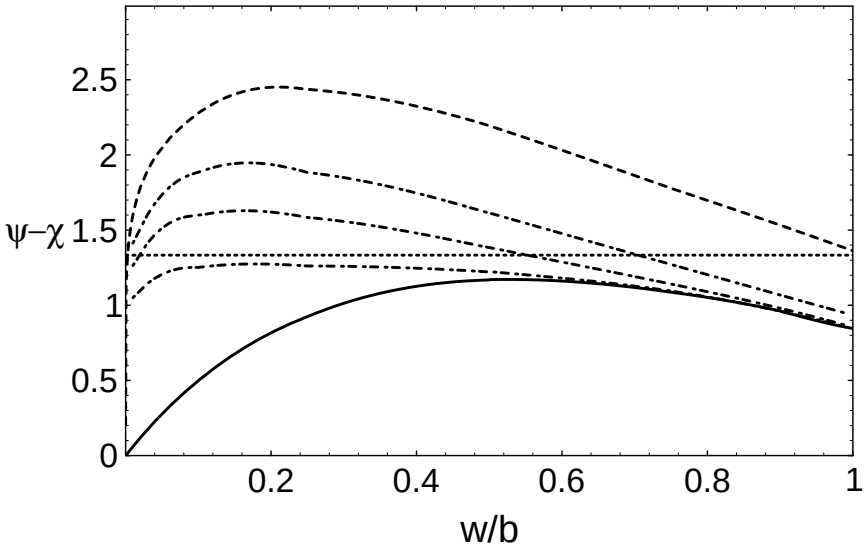

Figure 2: Difference of the polarizabilities (in units of b^3) of an annular cut versus its relative width w/b for different thicknesses of the wall $t = 0$; $w/2$; w; $2w$, and $t \gg w$ (from top to bottom). The dotted line corresponds to the circular hole in a thin wall, $(\psi - \chi)/b^3 = 4/3$.

the polarizabilities are [15]

$$\alpha_e = \frac{2\pi abc}{3I_b} \ , \tag{46}$$

and

$$\alpha_m = \frac{2\pi abc}{3(I_c - 1)} \ , \tag{47}$$

where

$$I_b = \frac{abc}{2} \int_0^\infty \frac{ds}{(s+b^2)^{3/2}(s+a^2)^{1/2}(s+c^2)^{1/2}} \ , \tag{48}$$

and I_c is given by Eq. (48) with b and c interchanged.

In the particular case $a = c$, $b = h$ we have an ellipsoid of revolution, and the polarizabilities are expressed in terms of the hypergeometric function ${}_2F_1$:

$$\alpha_e = \frac{2\pi a^2 h}{{}_2F_1(1,1;5/2;1-h^2/a^2)} \ , \tag{49}$$

and

$$\alpha_m = \frac{2\pi a^2 h}{{}_2F_1(1,1;5/2;1-a^2/h^2) - 3} \ . \tag{50}$$

5.3.1 Post

In the limit $a = c \ll h$, corresponding to a pinlike obstacle, we get a simple expression for the inductive impedance of a narrow pin (post) of height h and radius a, protruding radially into the beam pipe:[1]

$$Z(k) \simeq -ikZ_0 \frac{h^3}{6\pi R^2 \left(\ln(2h/a) - 1\right)} \ . \tag{51}$$

[1] One could use the known result for the induced electric dipole of a narrow cylinder parallel to the electric field [23]. It will only change $\ln(2h/a) - 1$ in Eq. (51) to $\ln(4h/a) - 7/3$.

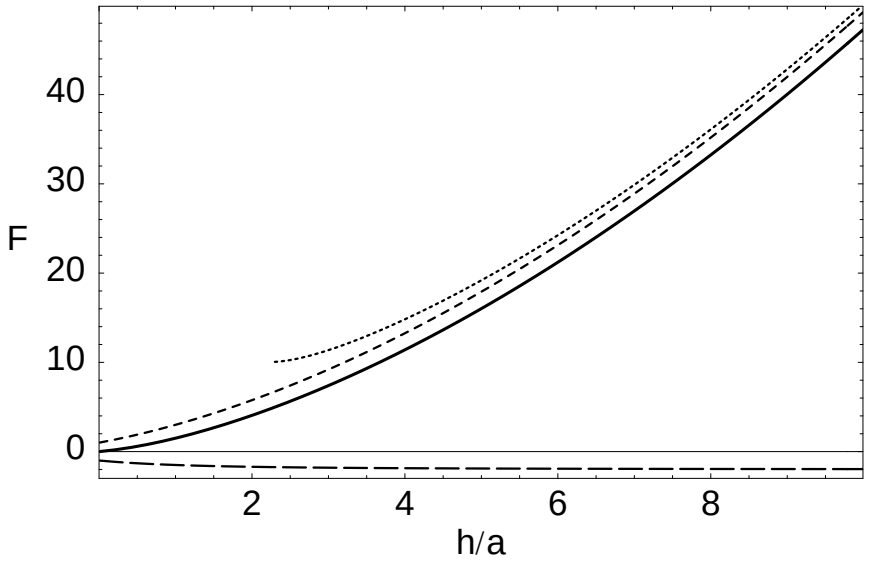

Figure 3: Function $F \equiv (\alpha_e + \alpha_m)/V$ versus aspect ratio h/a for a pinlike obstacle (solid line). The electric contribution is short dashed, the magnetic one is long dashed, and the dotted line shows the asymptotic form used in Eq. (51).

The factor $F \equiv (\alpha_e + \alpha_m)/V$, where $V = 2\pi a^2 h/3$ is the volume occupied by the obstacle, is plotted in Fig. 3 versus the ratio h/a. The figure also shows comparison with the asymptotic approximation given by Eq. (51).

5.3.2 Mask

One more particular case of interest is $h = a$, i.e. a semispherical obstacle of radius a. From Eqs. (49)-(50) the impedance of such a discontinuity is

$$Z(k) = -ikZ_0 \frac{a^3}{4\pi R^2} \ , \tag{52}$$

which is $3\pi/2$ times that for a circular hole of the same radius in a thin wall, cf. Eq. (42).

Another useful result that can be derived from the general solution, Eqs. (46)-(48), is the impedance of a mask intended to intercept synchrotron radiation. We put $b = c = h$, so that our model mask has the semicircular shape with radius h in its largest transverse cross section. Then the integral in Eq. (48) is reduced to

$$I_b = I_c = \frac{1}{3}\, {}_2F_1\left(1, \frac{1}{2}; \frac{5}{2}; 1 - \frac{h^2}{a^2}\right) \ ,$$

and we can further simplify the result for two particular cases.

The first one is the thin mask, $a \ll h$, in which case $\alpha_e \simeq 8h^3/3$, and again it dominates the magnetic term, $\alpha_m \simeq -V = -2\pi a h^2/3$. The coupling impedance for such an obstacle — a half disk of radius h and thickness $2a$, $a \ll h$, transverse to the chamber axis — is therefore

$$Z(k) = -ikZ_0 \frac{2h^3}{3\pi^2 R^2} \left[1 + \left(\frac{4}{\pi} - \frac{\pi}{4}\right)\frac{a}{h} + \dots\right] \ , \tag{53}$$

where the next-to-leading term is shown explicitly.

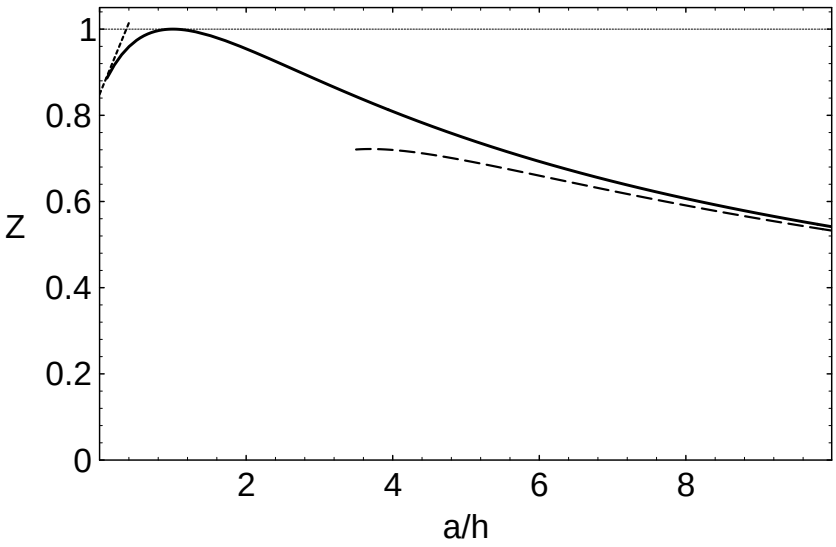

Figure 4: Impedance Z of a mask (in units of that for a semisphere with the same depth, Eq. (52) with $a = h$) versus its length. The narrow-mask approximation, Eq. (53), is short dashed, and the long-mask one, Eq. (54), is long dashed.

In the opposite limit, $h \ll a$, which corresponds to a long (along the beam) mask, the leading terms $\alpha_e \simeq -\alpha_m \simeq 4\pi a h^2/3$ cancel each other. As a result, the impedance of a long mask with length $l = 2a$ and height h, $h \ll l$, is

$$Z(k) \simeq -ikZ_0 \frac{4h^4}{3\pi R^2 l} \left(\ln \frac{l}{h} - 1 \right) , \tag{54}$$

which is relatively small due to the "aerodynamic" shape of this obstacle, in complete analogy with results for long elliptic slots [3, 4, 13].

Figure 4 shows the impedance of a mask with a given semicircular transverse cross section of radius h versus its normalized half length, a/h. The comparison with the asymptotic approximations Eqs. (53) and (54) is also shown. One can see, that the asymptotic behavior (54) starts to work well only for very long masks, namely, when $l = 2a \geq 10h$. Figure 4 demonstrates that the mask impedance depends rather weakly on the length. Even a very thin mask ($a \ll h$) contributes as much as $8/(3\pi) \simeq 0.85$ times the semisphere ($a = h$) impedance, Eq. (52), while for long masks the impedance decreases slowly: at $l/h = 20$, it is still 0.54 of that for the semisphere.

In practice, however, the mask has usually an abrupt cut toward the incident synchrotron radiation, so that it is rather one-half of a long mask. From considerations above one can suggest as a reasonable impedance estimate for such a discontinuity the half sum of the impedances given by Eqs. (53) and (54). This estimate is corroborated by 3D numerical simulations using the MAFIA code, at least, for the masks which are not too long. In fact, the low-frequency impedances of a semisphere and a half semisphere of the same depth — which can be considered as a relatively short realistic mask — were found numerically to be almost equal (within the errors), and close to that for a longer half mask. From these results one can conclude that a good estimate for the mask impedance is given simply by Eq. (52).

5.4 Axisymmetric Discontinuities

Following a similar procedure one can also easily obtain the results for axisymmetric irises having a semi-elliptic profile in the longitudinal chamber cross section, with depth $b = h$ and length $2a$ along the beam. For that purpose, one should consider limit $c \to \infty$ in Eq. (48) to calculate the effective polarizabilities $\tilde{\alpha}_e$ and $\tilde{\alpha}_m$ per unit length of the circumference of the chamber transverse cross section. The broad-band impedances of axisymmetric discontinuities have been studied in [10], and the longitudinal coupling impedance is given by

$$Z(k) = -ikZ_0 \frac{\tilde{\alpha}_e + \tilde{\alpha}_m}{2\pi R} \ , \tag{55}$$

quite similar to Eq. (40). As $c \to \infty$, the integral $I_c \to 0$, and I_b is expressed in elementary functions as

$$I_b = \frac{1}{2} {}_2F_1 \left(1, \frac{1}{2}; 2; 1 - \frac{h^2}{a^2}\right) = \frac{a}{a+h} \ .$$

It gives us immediately

$$\tilde{\alpha}_e = \frac{\pi}{2}\, h(h+a)\,; \qquad \tilde{\alpha}_m = -\frac{\pi}{2}\, ah \ , \tag{56}$$

and the resulting impedance of the iris of depth h with the semielliptic profile is simply

$$Z(k) = -ikZ_0 \frac{h^2}{4R} \ , \tag{57}$$

which proves to be independent of the iris thickness a. The same result has been obtained using another method [24], and also directly by conformal mapping in [15], following the general method of [10].

Using a conformal mapping, one can readily obtain an answer also for irises having the profile shaped as a circle segment with the chord of length s along the chamber wall in the longitudinal direction, and opening angle 2φ, where $0 \le \varphi \le \pi$. The impedance of such an exotic iris, expressed in terms of its height $h = s(1 - \cos\varphi)/(2\sin\varphi)$:

$$\begin{aligned} Z(k) &= -ikZ_0 \frac{h^2}{2R(1-\cos\varphi)^2} \times \\ &\times \left[\frac{\varphi(2\pi-\varphi)}{3(\pi-\varphi)^2} \sin^2\varphi - \frac{2\varphi - \sin 2\varphi}{2\pi}\right] \ . \end{aligned} \tag{58}$$

Again, the impedance is proportional to h^2, but the coefficient now depends (in fact, rather weakly) on φ.

A few useful results for low-frequency impedances of axisymmetric cavities and irises with a rectangular, trapezoidal and triangular transverse profile have been obtained in [10] using conformal mapping to calculate the electric polarizability.

The low-frequency impedance of the small short pill-box whose length g is not large than depth h is

$$Z(\omega) = -ikZ_0 \frac{1}{2\pi R} \left(gh - \frac{g^2}{2\pi}\right) \ , \tag{59}$$

The low-frequency impedance of the shallow enlargement takes the form

$$Z(\omega) = -ikZ_0 \frac{h^2}{2\pi^2 R} \left(2\ln(2\pi g/h) + 1\right) \ , \tag{60}$$

where $g \gg h$, but still less than R.

The low-frequency impedance of a small step of depth $h \ll R$ is

$$Z(\omega) = -ikZ_0 \frac{h^2}{4\pi^2 R} \left(2\ln(2\pi R/h) + 1\right) \ . \tag{61}$$

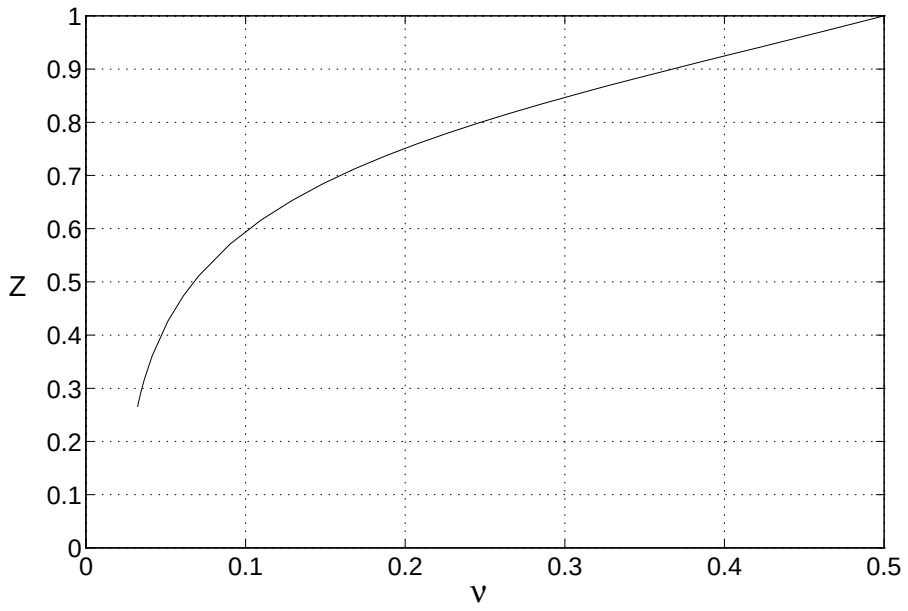

Figure 5: Impedance Z of a transition versus its slop, in units of that for the abrupt step ($\nu = 1/2$, Eq. (61)) with the same height.

The inductance produced by the transition with the slope angle $\theta = \pi\nu$ has the form:

$$Z(\omega) = -i\frac{Z_0 k h^2}{2\pi^2 R}\left\{\ln\left[\pi\nu\left(\frac{b}{h} - 2\cot\pi\nu\right)\right] + \frac{3}{2} - \gamma - \psi(\nu) - \frac{\pi}{2}\cot\pi\nu - \frac{1}{2\nu}\right\}, \tag{62}$$

where $\gamma = 0.5772\ldots$ is Euler's constant, $\psi(\nu)$ is the psi-function and the transition is assumed to be short compared to the chamber radius, i.e. transition length $l = h\cot\pi\nu \ll R$. The ratio of this inductance to that of the abrupt step ($\nu = 1/2$, Eq. (61)) with the same height is plotted in Fig. 5 as a function of the slope angle.

The impedance of a thin (or deep) iris, $g \ll h$, has the form

$$Z(\omega) = -ikZ_0\frac{1}{4R}\left[h^2 + \frac{gh}{\pi}\left(\ln(8\pi g/h) - 3\right)\right] . \tag{63}$$

This formula works well even for rather large h, when h is close to R.

More generally, the low-frequency impedance of the iris having a rectangular profile with an arbitrary aspect ratio is

$$Z(\omega) = -ikZ_0\frac{gh}{2\pi R}F\left(\frac{h}{g}\right) , \tag{64}$$

where function F(x) is plotted in Fig. 6.

The impedances of discontinuities having a triangle-shaped cross section with height (depth) h and base g along the beam are given below. When $g \ll h$, the low-frequency impedance of a triangular enlargement is

$$Z(\omega) = -ikZ_0\frac{1}{4\pi R}\left(gh - \frac{g^2}{\pi}\right) , \tag{65}$$

and that of a triangular iris is

$$Z(\omega) = -ikZ_0\frac{1}{4R}\left[h^2 + \frac{2gh}{\pi}(1 - \ln 2)\right] . \tag{66}$$

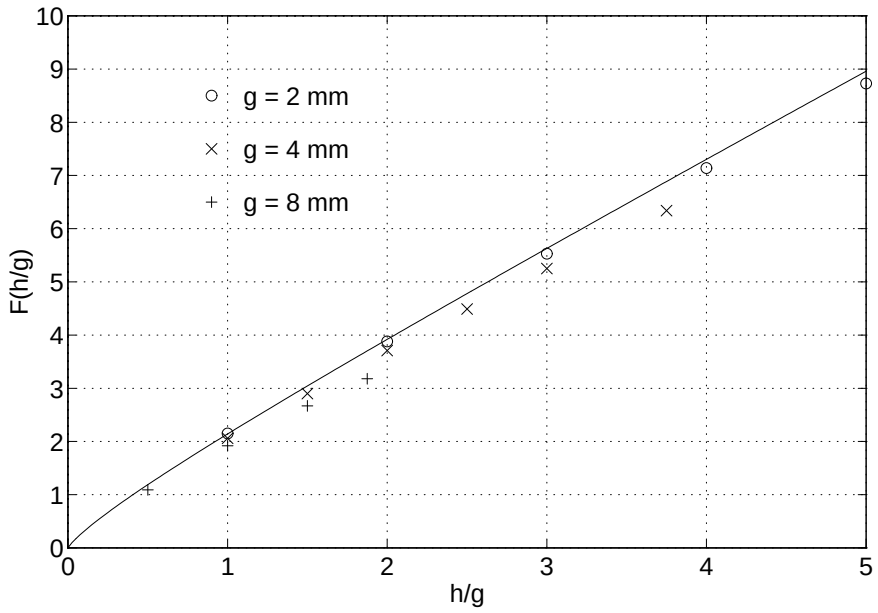

Figure 6: The inductance dependence on the aspect ratio of a rectangular iris, cf. Eq. (64). The marks show numerical results for a beam pipe with radius $R = 2$ cm, for comparison.

For the case of shallow triangular perturbations, $h \ll g < R$, both the enlargement and contraction of the chamber have the same inductance,

$$Z(\omega) = -ikZ_0 \frac{h^2 2 \ln 2}{\pi^2 R} \ , \tag{67}$$

which is independent of g.

Appendix

Circular Chamber

For a circular cross section of radius b the eigenvalues $k_{nm} = \mu_{nm}/b$, where μ_{nm} is mth zero of the Bessel function $J_n(x)$, and the normalized EFs are

$$e_{nm}(r,\varphi) = \frac{J_n(k_{nm}r)}{\sqrt{N^E_{nm}}} \left\{ \begin{array}{c} \cos n\varphi \\ \sin n\varphi \end{array} \right\} \ , \tag{68}$$

with $N^E_{nm} = \pi b^2 \epsilon_n J^2_{n+1}(\mu_{nm})/2$, where $\epsilon_0 = 2$ and $\epsilon_n = 1$ for $n \neq 0$. For TE-modes, $k'_{nm} = \mu'_{nm}/b$ with $J'_n(\mu'_{nm}) = 0$, and

$$h_{nm}(r,\varphi) = \frac{J_n(k'_{nm}r)}{\sqrt{N^H_{nm}}} \left\{ \begin{array}{c} \cos n\varphi \\ \sin n\varphi \end{array} \right\} \ , \tag{69}$$

where $N^H_{nm} = \pi b^2 \epsilon_n (1 - n^2/\mu'^2_{nm}) J^2_n(\mu'_{nm})/2$. In this case $\tilde{e}_\nu = 1/(2\pi b)$, which also follows from the Gauss law, and the formula for the inductive impedance takes an especially simple form, cf. [3, 4].

Rectangular Chamber

For a rectangular chamber of width a and height b the eigenvalues are $k_{nm} = \pi\sqrt{n^2/a^2 + m^2/b^2}$ with $n, m = 1, 2, \ldots$, and the normalized EFs are

$$e_{nm}(x, y) = \frac{2}{\sqrt{ab}} \sin\frac{\pi n x}{a} \sin\frac{\pi m y}{b} \ , \tag{70}$$

with $0 \le x \le a$ and $0 \le y \le b$. Let a hole be located in the side wall at $x = a,\ y = y_h$. From Eq. (3) after some algebra follows

$$\tilde{e}_\nu = \frac{1}{b}\Sigma\left(\frac{a}{b}, \frac{y_h}{b}\right) \ , \tag{71}$$

where

$$\Sigma(u, v) = \sum_{l=0}^{\infty} \frac{(-1)^l \sin[\pi(2l+1)v]}{\cosh[\pi(2l+1)u/2]} \tag{72}$$

is a fast converging series; the behavior of $\Sigma(u, v)$ versus v for different values of the aspect ratio u is plotted in Ref. [5].

6 Summary

A review of calculating the beam coupling impedances of small discontinuities was presented. We also collected some analytical formulas for the inductive contributions due to various small obstacles to the beam coupling impedances of the vacuum chamber.

An importance of understanding these effects can be illustrated by the following example. An original design of the beam liner for the LHC vacuum chamber anticipated a circular liner with many circular holes of 2-mm radius, providing the pumping area about 5% of the liner surface. Their total contribution to the low-frequency coupling impedance was calculated [3] to be

$$|Z/n| = 0.53\ \Omega, \qquad |Z_\perp| = 20\ M\Omega/m\,,$$

which was close or above (for $Z_\perp$) the estimated instability threshold. A modified liner design had about the same pumping area provided by rounded-end slots 1.5×6 mm^2, which were placed near the corners of the rounded-square cross section of the liner [7]. As a result of these changes, the coupling impedances were reduced by more than an order of magnitude, 30-50 times:

$$|Z/n| = 0.017\ \Omega, \qquad |Z_\perp| = 0.4\ M\Omega/m\,.$$

Now the pumping slots are not among the major contributors to the impedance budget of the machine.

One should mention that these notes do not include more recent developments, in particular, results for coaxial structures, frequency corrections for polarizabilities, etc. Some of these new results and proper references can be found in [16].

References

[1] H.A. Bethe, "Theory of diffraction by small holes," Phys. Rev. **66**, 163 (1944).

[2] R.E. Collin, *Field Theory of Guided Waves* (IEEE Press, NY, 1991).

[3] S.S. Kurennoy, "Coupling impedance of pumping holes," Part. Acc. **39**, 1 (1992); also CERN Report SL/91-29(AP)rev, Geneva (1991)

[4] R.L. Gluckstern, "Coupling impedance of a single hole in a thick-wall beam pipe," Phys. Rev. A **46**, 1106 and 1110 (1992).

[5] S.S. Kurennoy, "Beam interaction with pumping holes in vacuum-chamber walls," in Proceed. of EPAC (Berlin, 1992), p.871; Report IHEP 92-84, Protvino, 1992.

[6] S.S. Kurennoy, "Beam-chamber coupling impedance. Calculation methods," CERN Report SL/91-31(AP), Geneva (1991); also Phys. Part. Nucl. **24**, 380 (1993).

[7] S.S. Kurennoy, "Impedance issues for LHC beam screen," Part. Acc. **50**, 167 (1995).

[8] G.V. Stupakov, "Coupling impedance of a long slot and an array of slots in a circular vacuum chamber," Phys. Rev. E **51**, 3515 (1995).

[9] S.S. Kurennoy, R.L. Gluckstern, and G.V. Stupakov, "Coupling impedances of small discontinuities: A general approach," Phys. Rev. E **52**, 4354 (1995).

[10] S.S. Kurennoy and G.V. Stupakov, "A new method for calculation of low frequency coupling impedance," Part. Acc. **45**, 95 (1994).

[11] R.L. Gluckstern and J.A. Diamond, "Penetration of fields through a circular hole in a wall of finite thickness," IEEE Trans. MTT **39**, 274 (1991).

[12] B. Radak and R.L. Gluckstern, "Penetration of fields through an elliptical hole in a wall of finite thickness," IEEE Trans. MTT **43**, 194 (1995).

[13] S.S. Kurennoy, "Pumping slots: coupling impedance calculations and estimates," Report SSCL-636, Dallas (1993) (unpublished).

[14] S.S. Kurennoy, "Polarizabilities of an annular cut in the wall of an arbitrary thickness," IEEE Trans. MTT **44**, 1109 (1996).

[15] S.S. Kurennoy, "Beam coupling impedances of obstacles protruding into a beam pipe," Phys. Rev. E **55**, 3529 (1997).

[16] *Handbook of Accelerator Physics and Engineering*, A.W. Chao and M. Tigner, Eds. (World Scientific, Singapore, 1999), Sect. 3.2.

[17] P.M. Morse and H. Feshbach, *Methods of Theoretical Physics* (McGraw-Hill, NY, 1953), § 6.3.

[18] G.V. Stupakov and S.S. Kurennoy, "Trapped electromagnetic modes in a waveguide with a small discontinuity," Phys. Rev. E **49**, 794 (1994).

[19] S.S. Kurennoy, "Trapped modes in waveguides with many small discontinuities," Phys. Rev. E **51**, 2498 (1995).

[20] F. Caspers and T. Scholz, "Measurement of trapped modes in perforated waveguides," Part. Acc. **51**, 251 (1995).

[21] S.S. Kurennoy and Y.H. Chin, "Impedances and power losses due to pumping slots in B-factories," Part. Acc. **52**, 201 (1996).

[22] S.S. Kurennoy, "Impedances and Power Losses for an Off-Axis Beam", in Proceed. of EPAC (Barcelona, 1996), p.1449.

[23] L.D. Landau and I.M. Lifshitz, *Electrodynamics of Continuous Media* (Pergamon Press, Oxford, 1960), §3.

[24] R.L. Gluckstern and S.S. Kurennoy, "Coupling impedances of axisymmetric irises and cavities with semi-elliptical profile in a beam pipe," Phys. Rev. E **55**, 3533 (1997).